GEOL492 notes 2025/26

Use of “Time Fields” and “Resistance Fields” for analysis and inversion of refraction seismic and resistivity data

Igor Morozov

igor.morozov@usask.ca

Introduction

Geophysical data almost always require extensive data analysis before any geological or engineering interpretation can be made. Generally, this analysis includes four major steps:

I) Checking for various acquisition errors and noises in the data and editing the records to correct for these errors and reduce noise.

II) Transformations of the data and their presentation in multiple forms emphasizing certain targets or aspects of the data. For example, sorting seismic records into common-midpoint gathers allows analyzing specific areas within the subsurface. Band-pass or spatial filtering of seismic waveforms or gravity readings allow reducing the noise and reveal targets in depth. Such transformations may also include numerous “corrections” removing undesirable effects from the data, such as static corrections in seismic work or drift, free-air, and other corrections of gravity measurements.

III) Presentation of the data in various forms, such as by dependencies on the source, receiver or mid-point locations, or source-receiver distances.

IV) The final step is data inversion, which consists of applying multiple algorithms or manual interpretation methods. These inversion methods are often strongly dependent on how the data are sorted, filtered, and transformed.

Among the various geophysical disciplines, seismic data analysis involves by far the largest volumes of data and offers the greatest variety of methods in all steps I) –IV) above. In the first part of this project, we study one of such methods for refraction travel-time analysis called the “Travel-Time Field” (TTF). This simple and elegant method was developed for deep seismic investigations in 1970-80s (Novotný, 1988). Later, it was applied by Morozov et al. (2005) and Jhajhria and Morozov (2013) but unfortunately seems to be still little used since then. We apply this method to the analysis of a near-surface refraction seismic profile acquired during the 2025 UofS field school.

In the second part of the project, we point out an important analogy between seismic travel-time and resistivity data. This analogy allows greatly improving the resistivity data analysis using the experience from seismic work. We show that a “Resistance Field” (RF) can be constructed similarly to the TTF, yielding numerous advantages for all data analysis steps I) –IV). In particular, derivation of an RF leads to a new approach to correcting for reciprocity and several significantly improved resistivity inversion methods. To our knowledge, the concept of RF has not been used in application to resistivity imaging, or at least not mentioned in mainstream textbooks (e.g., Reynolds, 2011).

In the following sections, I will first describe the methods of travel-time and resistivity fields and then apply them to 2-D refraction and 3-D resistivity data collected during the 2025 geophysics field schools (Morozov, 2025).

Seismic Travel-Time Fields

Although seismic travel times are measured at discrete positions of receivers, they usually represent sampling of contiguous intervals within which certain types of wave arrive at the surface: direct or refracted (head) waves, reflected from certain horizons or scatterers in the subsurface, or surface waves. For a given seismic phase, these piecewise-continuous functions of source and receiver coordinates represent the travel-time field (TTF). For first-arrival travel times, the TTF is usually (in the absence of low-velocity layers) a continuous function of all spatial coordinates.

For a single seismic line (2-D seismic imaging), the TTF function can be viewed as a 2-D surface in the 3-D space of (*source coordinate*, *receiver coordinate*, *travel time*). Due to travel-time reciprocity (section below), this surface is always symmetric in the offset direction, and this property can be used to extract the source and receiver station static corrections. Most importantly, for a 2-D survey the travel-time field can be well sampled by the picks, allowing a direct interpolation of the time field.

Figure 1 shows how such 2-D TTF was constructed for a deep crustal marine-land survey in British Columbia. In this Figure, each pair of slanting lines represent first-arrival travel-time picks performed at one of the 29 receiving stations from numerous air-gun shots along the fjord. Lines slanting upward to the right are graphs of the first-arrival times for waves travelling forward along the profile, and the lines slanting upward-left are reversed recordings. Most importantly, the travel-time picks in Figure 1 are plotted against the *midpoints* between the sources and receivers, so that by the condition of reciprocity, for any pair of receivers R_1 and R_2 the graphs must intersect exactly halfway between them. Due to this property, all recorded travel times represent a function of the midpoint coordinate and source-receiver offset. This surface is the TTF. It can be interpolated in the (midpoint,offset) plane and plotted in colour, by contouring, or by 3-D perspective plots (Figure 2).

The slanting lines in Figure 1 (perfectly straight in Figure 2) are the *common-receiver travel times* corresponding to data points for which $x_R = const$. By connecting points with fixed source-receiver offsets, graphs of *common-offset travel times* are obtained (near-horizontal lines in Figure 1). Note that in Figure 2, the general change of colour in the offset (vertical) direction shows the variation of velocity with depth and the criss-crossing patterns of short-scale variations are due to the shallow velocity variations and statics.

By using the TTF, results of experiments different from the actual seismic acquisition can be predicted without knowing anything about the subsurface velocity structure. For example, if we extract a vertical cross-section from the surfaces in Figures 1 or 2, a *common-midpoint travel-time curve* is obtained (Figure 3). The shape of this curve can be inverted for 1-D layering beneath this midpoint. This estimation can be

repeated at every midpoint, giving a detailed subsurface velocity structure (Novotný, 1988).

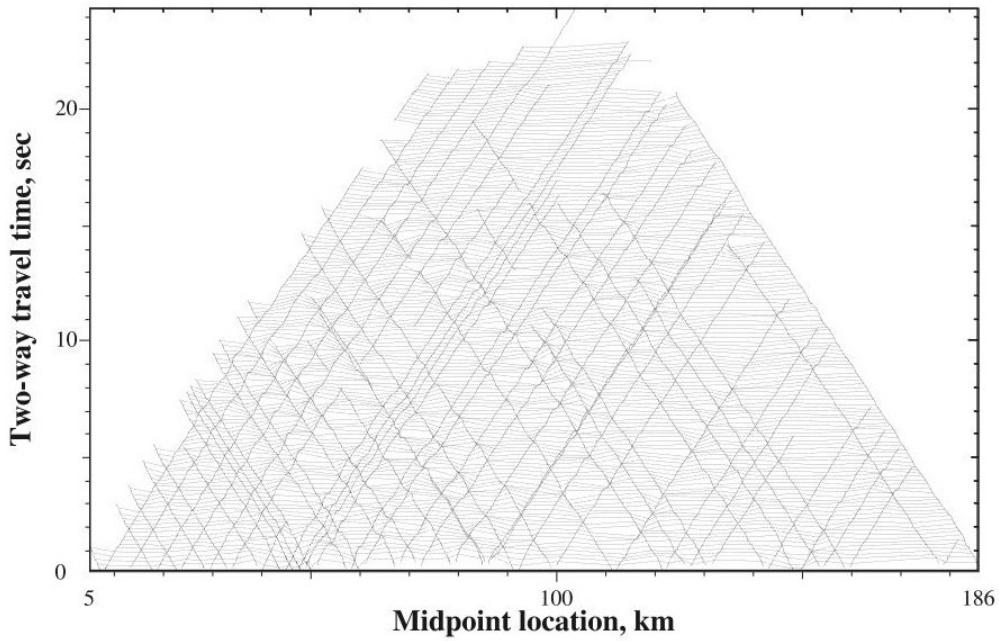

Figure 1. Construction of the first-arrival TTF for one refraction line from a deep crustal dataset ACCRETE (1998; airgun line along the Portland Canal fjord along the border of Alaska (USA) and British Columbia (Canada).

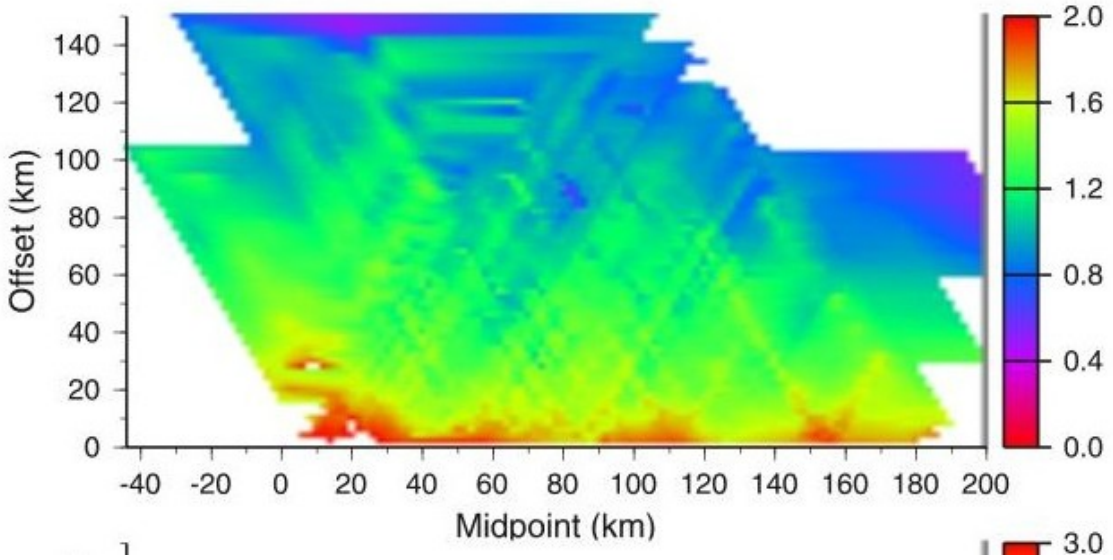

Figure 2. TTF from another set of ACCRETE shots interpolated in the (*midpoint*,*offset*) plane. Colour shows the reduced travel time $t_{red} = t - offset/V_R$, where V_R = 6.0 km/s is the reduction velocity.

For a 3-D refraction or reflection seismic dataset recorded on the Earth's surface, there are two independent source coordinates (x_S, y_S) and two receiver coordinates (x_R, y_R). Therefore, the TTF is a 4-D surface in a 5-D space (x_S, y_S, x_R, y_R, t). It is convenient to plot and analyze this surface by 2-D "slices" taken at common sources $(x_S, y_S) = const$, common receivers $(x_R\, y_R) = const$, or common midpoints $\frac{1}{2}(x_S + x_R, y_S + y_R) = const$.

Here is an assignment: Sketch and place here a schematic curve of *travel_time*(*distance*) dependence for first arrivals in a 3-layer velocity model like in geol335 labs.

Label moveouts 1/*V* and crossover distances x_c.

Make arrivals start from nonzero time at x = 0 and label that time Δt_S

Figure 3. Schematic illustration of first-arrival travel times in a layered model with layer velocities V_i increasing with depth. From the slopes and cross-over distances x_c of the travel-time segments, layer velocities and depths are estimated. Time Δ_{tS} is the source static or uphole time.

If a sufficiently dense source-receiver sampling is available, the TTF can be derived directly from the data by decomposing it into a spatially "smooth" TTF $t_0(S_i, R_j)$ which would have been recorded for sources and receivers located on the surface of a relatively smooth velocity structure, plus additive terms specific to each source and receiver:

$$t(S_i, R_j) = t_0(S_i, R_j) + \Delta t(S_i) + \Delta t(R_j), \qquad (1)$$

where S_i is the i^{th} source and R_j is the j^{th} receiver in the seismic survey. The additive times describe the highly variable effects of the shallow subsurface which are not sampled by the available offset range and density of source and receiver coverage (Figure 3). These

additive terms are called “static times” or “statics”, and also “uphole times” for seismic sources placed in boreholes. These terms are also called the “short-wavelength statics” (because they vary arbitrarily for each shot or receiver) in Hampson-Russell GLI3D program for refraction statics analysis (now included in GeoTomo software).

The statics-corrected corrected TTF $t_0(S_i, R_j)$ possesses an important property of the source-receiver reciprocity:

$$t_0(S_i, R_j) = t_0(R_j, S_i). \qquad (2)$$

This relation means that when a source and a receiver are switched places, the travel time between them must remain the same. Using this property, eq. (1) can be solved for $\Delta t(S_i)$ and $\Delta t(R_j)$ purely from the data, without assuming any velocity structure and modelling seismic wave propagation.

Resistance Fields

The concept of TTF has a straightforward analog in electrical resistivity studies, which can be called the Resistance Field (RF) or resistance-matrix field. Similarly to Figure 3, consider a single source point (current-injection electrode A) and a single receiver point (potential electrode M) which, however, are supposed to be one of many other recordings at adjacent points. Since another pair of electrodes is always required for resistivity measurements (injection current sink B and potential N), let us place them at the infinity, where the potential equals zero. This combination of electrodes is called the pole-pole array.

For a pole-pole array, the resistance of the circuit between electrodes A and M is

$$R(A, M) = \frac{V(MN)}{I(AB)}. \qquad (3)$$

Similar to the TTF (eq. (1)), this resistance is a function of two pairs of coordinates of points A and M: $R(x_A, y_A, x_M, y_M)$ and therefore it can be viewed as a 4-D surface in a 5-D space of coordinates (x_A, y_A, x_M, y_M, R). Similar to eq. (1), the near-electrode effects can be approximated by contact resistances for $\Delta R(A_i)$ and $\Delta R(M_j)$, and a “surface-

consistent" resistance function $R_0(A_i, M_j)$ obtained:

$$R(A_i, M_j) = R_0(A_i, M_j) + \Delta R(A_i) + \Delta R(M_j). \quad (4)$$

In Figure 4, this function $R_0(A_i, M_j)$ is shown schematically as a function of the source-receiver distance r_{AM}. Instead of the linear travel-time segments in the seismic TTF (Figure 3) the characteristic shape of the RF is close to 1/*distance*. Also similar to the TTF reciprocity (eq. 2), the corrected RF satisfies the reciprocity relation

$$R_0(A_i, M_j) = R_0(M_j, A_i). \quad (5)$$

Sketch a s schematic curve for *resistance*(*distance_from_source*) for a pole-pole resistivity survey.

Figure 4. Schematic distance dependence of resistance measured using a pole-pole array.

Reciprocity Correction

Relations (1) and (4) lead to useful tools for travel-time or resistivity analysis in large and densely sampled datasets. A key initial step of this analysis consists in checking how well the recorded data satisfy the reciprocity conditions and correcting for any mismatches in them. Note that correct reciprocity is extremely important for both travel-time and resistivity data because data violating this condition *cannot* be interpreted in terms of a subsurface structure. Mismatches in data reciprocity propagate into the model and appear as spurious structures within the subsurface. Thus, reciprocity must be accurately enforced in any data before performing any type of inversion.

Using the first-arrival travel-time problem as an example, consider a 3-D dataset and assume that we have some algorithm *F*(...) allowing to: 1) subtract the current estimates of the source and receiver terms in eq. (1), and 2) interpolate the subtracted data at an arbitrary source location S_i and receiver location R_j:

$$\tilde{t}_0(S_i, R_j) = F\left(S_i, R_j; t^{obs} - \Delta t(S) - \Delta t(R)\right). \qquad (6)$$

This quantity is the current estimate of the corrected TTF $t_0(S_i, R_j)$. Because arguments S_i and R_j of this function are arbitrary surface coordinates but not the specific source and receivers, $t_0(S_i, R_j)$ is called the "surface-consistent" model for travel times.

Subtracting from $t_0(S_i, R_j)$ its values with the source and receiver switched places, we obtain the reciprocity error:

$$\delta_{rec}(S_i, R_j) = \tilde{t}_0(S_i, R_j) - \tilde{t}_0(R_j, S_i) = 0. \qquad (7)$$

This error must equal zero for all *i* and *j*. Equations (6) and (7) give an inverse problem from which we can determine vectors $\Delta t(S)$ and $\Delta t(R)$. Note that this inversion contains an ambiguity because equations (6) are invariant with respect to adding an arbitrary constant to all $\Delta t(S_i)$ and subtracting the same constant from all $\Delta t(R_j)$. This ambiguity can be removed by adding an additional requirement that $t_0(S_i, R_j) \to 0$ when $R_j \to S_i$. For the RF case, this additional condition will be $R_0(A_i, B_j) \to 0$ when $R_j \to \infty$ or $S_i \to \infty$.

For the RF case, the "data interpolation" (i.e., approximate data-fitting) equation is different. In a practical electrical measurement, two current electrodes A, B and two potential electrodes M, N are always used, and the basic quantity measured in the experiment is the cross-resistance (ratio of the voltage between M and N to the current from A to B):

$$R_{AB,MN} = \frac{V_{MN}}{I_{AB}} = R_0(A, M) - R_0(A, N) - R_0(B, M) + R_0(B, N). \qquad (8)$$

In this equation, function $R_0(P_1, P_2)$ is defined for arbitrary points P_1 and P_2 and plays the role of the interpolation function *F*(...) above. Note that the contact-resistance terms $\Delta R(A_i)$ and $\Delta R(M_j)$ in eq. (4) are cancelled out in this 4-electrode measurement. The

measured cross-resistance in the left-hand side of eq. (8) is related to the apparent resistivity usually reported for the electrode array:

$$\rho_a = kR_{AB,MN}, \qquad (9)$$

where k is the geometric factor for the array. For instance, for an ordinary Wenner ("α") array, $k = 2\pi a$, where a is the spacing between each pair of electrodes in the sequence A - M - N - B.

Equations (8) can be inverted for all data by selecting a suitable parametrization of function $R_0(P_1, P_2)$ by a relatively small number of parameters analogously to eq. (6) for TTF. Finding this parametrization is the principal task of this project, and it can be achieved by using basis functions described in the next section. Also similar to the case of the TTF (eq. 6), the inverse problem in eq. (8) is "under-constrained" because all data readings are limited to double differences between pairs of electrodes. This difficulty can be remedied by using "regularization" or "damping" of the inverse, or using the so-called "prior constraints" or other methods.

The interpolation and solution procedure in eqs. (6) - (8) may be nonlinear, and therefore they need to be iterated until a suitable solution for vectors $\Delta t(S)$ and $\Delta t(R)$ or function $R_0(A, M)$ is obtained.

TTF or RF interpolation

The interpolation procedure for functions $F(...)$ or $R_0(...)$ required for solving eqs. (6) or (8) needs to be performed carefully. For seismic TTFs, cross-over distances need to be determined first and linear or slightly nonlinear interpolation can then likely be used between these distances (Figure 3). For RF, since the principal dependence of resistance on distance r between electrodes A and M is $R_0(r) \approx const/r$ (Figure 4), it is better to interpolate the product $y(r) = r\,R(r)$. Note that this product is proportional to the apparent resistivity for the pole-pole array. The "static" contact-resistance shifts $\Delta t(S)$ and $\Delta t(R)$ will be represented by possible trends $y(r) \propto r$ near point r = 0, and therefore the interpolation should account for such trends. It is also important to ensure that the interpolated dependencies are smooth functions of both r and azimuth.

To perform the interpolation satisfying the above requirements, we split the range of distances $r \in \langle 0, r_{max} \rangle$ into several intervals and use the so-called Wiggins polynomial basis functions within them. These functions are of two kinds: one having the value of the basis function equal one at the central node (Figure 5, top) and another one with the value of zero but derivative equal one (bottom in the Figure). At the ends of the interval, both the values and derivatives of each Wiggins functions equal zero.

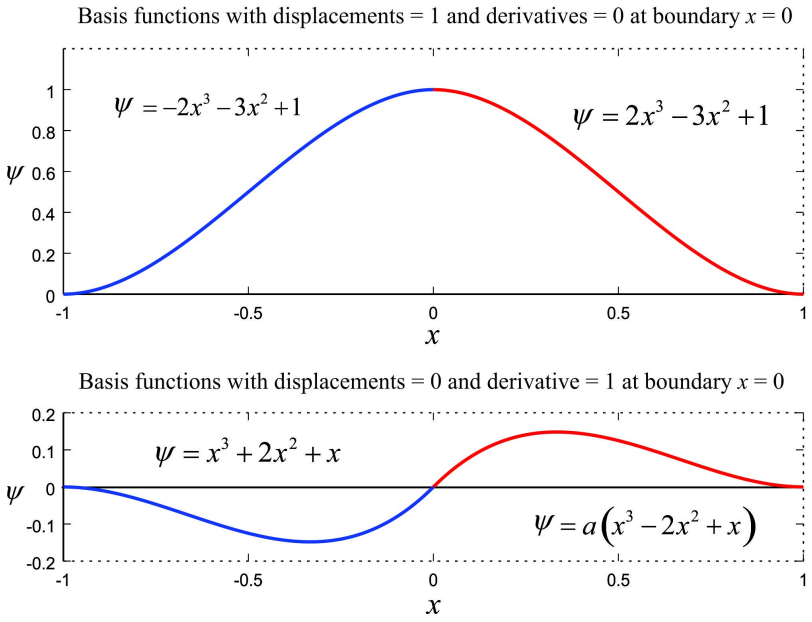

Figure 5.Two types of Wiggins (polynomial) basis functions in two intervals joining at point $x = 0$ (blue and red). These functions are often used for constructing layered Earth models in earthquake seismology, and they can be used for approximating smooth distance dependencies of the TTF or RF in this project.

New approach to inversion using TTF or RF

After the reciprocal-point corrected and surface-consistent TTF $t_0\langle S_i, R_j \rangle$ or RF $R_0\langle A_i, M_j \rangle$ is obtained, it can be used to implement new inversion approaches. The first of these approaches constrains the key features of the velocity or resistivity model without utilizing complex 3-D algorithms. This method was suggested for seismic TTFs by Novotný (1988). At several (or even each) midpoints selected within the study area, common-midpoint profiles will be extracted from the TTF (RF) traversing the study area

at several azimuths. The profiles will be examined by using 1-D inversion methods for locations of boundaries and velocity (or resistivity) variations, and the final model will be determined by comparing or merging these 1-D models. For the present shallow work, it will be particularly interesting to correlate the variations of the model with surface topography.

The second new inversion method applies specifically to resistivity or IP problems and utilize the inversion methodology accepted in this field. The usual approach to 2-D or 3-D multichannel resistivity inversion or ERT (electrical resistivity tomography) consists in extracting some suitable 4-electrode groups (AB,MN) from the data which would be spaced as uniformly as possible, have similar orientations, and contain a range of dimensions covering the target depths. Unfortunately, this selection is practically impossible with real data because the existing 3-D arrays are usually irregular in shapes and strongly biased toward shorter electrode spacings.

The RF method allows us to resolve the above problem and produce a perfectly regular set of "virtual" (AB,MN) arrays with controlled densities of sampling at any depth. Once the corrected RF $R_0(P_1, P_2)$ is derived for arbitrary locations P_1 and P_2, it can predict readings for arbitrary electrical-resistivity experiments in the area. Thus, we can construct a grid of equal-sized and regularily-spaced 4-electrode arrays directly from 3-D field resistivity data. These reciprocal-error free and regularly-spaced and shaped "virtual" data can be used to plot pseudo-depth volumes or invert them using standard inversion algorithms, ensuring good stability and quality of the inversion.

... need to add sections about results and conclusions ...

Conclusions

...

The improvement in the resistivity analysis method made in this work should also apply to the analysis and presentation of Induced Polarization (IP) data.

References

Jhajhria, A., Morozov, I. B. (2013), Refraction-static analysis in 3-D by using time fields, Can. J. Expl. Geoph., 38, 12-21

Morozov, I. B., Morozova, E. A., Smithson, S. B., Richards, P. G., Khalturin, V. I., and Solodilov, L. N. (2005). 3D First-arrival regional calibration model of northern Eurasia, Bulletin of the Seismological Society of America, Vol. 95, No. 3, pp. 951–964, June 2005, doi: 10.1785/0120030173

Morozov, I. (2025), GEOL487 course materials on UofS Canvas

Novotný, M., 1988. Linearized velocity inversion of refraction arrivals by iterative ray interpretation, in *Inverse modeling in exploration geophysics*, Friedr. Vieweg & Sohn, Brainschweig/Wiesbaden, pp. 417-432, eds. A. Vogel, R. Gorenflo, B. Kummer, and C. O. Ofoegbu.

Reynolds, J. M. (2011) An Introduction to Applied and Environmental Geophysics, 2-nd ed, John Willey & Sons